

Effect of hydrothermal treatment on the structure and foaming of waste glass

Uroš Hribar^{a,b,*}, Matjaž Spreitzer^a, Jakob König^a

^a Advanced Materials Department, Jožef Stefan Institute, Jamova cesta 39, 1000, Ljubljana, Slovenia

^b Jožef Stefan International Postgraduate School, Jamova cesta 39, 1000, Ljubljana, Slovenia

ARTICLE INFO

Keywords:

Foamed glass

Waste glass

Hydrothermal treatment

ABSTRACT

This study explores the potential of hydrothermally treated waste glass for producing foamed glass using a carbonaceous foaming agent (glycerol) in an air atmosphere. The objective was to assess the feasibility of this alternative route for producing sustainable, lightweight materials with reduced energy and material inputs by repurposing cathode ray tube panels (CRT), flint glass (FG), and mixed-color container glass (MCG). Investigated glass powders were treated in a saturated steam atmosphere inside a pressure vessel and characterized using X-ray diffraction and Fourier-transform spectroscopy to identify structural changes. The foaming behavior of hydrothermally treated waste was analyzed through heating stage microscopy and thermogravimetric analysis coupled with mass spectrometry. The foamed glass samples were further assessed for density and thermal conductivity.

The results demonstrate that hydrothermal treatment significantly influences the foaming process. Glass powders with higher content of structurally bonded water exhibit lower sintering temperature and pronounced expansion after the hydrothermal treatment. A higher hydration level reduced the onset foaming temperature and facilitated higher expansion. Additionally, combining hydrothermally treated powders with glycerol as a foaming agent enabled effective expansion, even in an air atmosphere, achieving density as low as 108 kg m^{-3} .

The results of this study suggest that hydrothermal treatment of waste glasses enables the implementation of carbonaceous foaming agents in the air atmosphere and could thus offer an alternative route for the foaming of glass.

1. Introduction

Lightweight materials in construction applications are beneficial from both ecological and economical perspective. Waste glass is a cheap and abundant raw input [1] for sustainable lightweight materials, and its reuse supports efforts to increase glass recycling.

Foamed glass is a highly porous material characterized by dimensional stability, resistance to corrosion and water, non-flammability, and resistance to bacteria [2]. This combination of properties is particularly useful for thermal insulation in construction, which is the main commercial application of foamed glass. Foamed glass is one of the alternative thermal insulation materials and a promising candidate to become a more common sustainable material in the future, especially due to its longevity and possibility of being produced from waste materials. The most common method for producing foamed glass, both commercially and scientifically studied, is the sintering process. The

process requires use of special foaming additives and a high energy input. Composition-dependent properties such as viscosity, surface tension, and glass stability will significantly affect the foaming process. High-quality foamed glass panels are produced industrially by adjusting the glass composition through re-melting and the use of additives [3]. The required energy input can be reduced by avoiding the glass re-melting step, however, thus eliminating the ability to adjust the composition of the raw waste glass. Additionally, the energy efficiency of the process and its environmental impact can be improved even further with the use of water glass [4] to enable foaming in the air atmosphere [5].

Silicate glasses are chemically inert and durable materials, which makes them commonly used in the packaging, construction, and automotive industries. However, even glasses with very high purity can contain traces of chemically bound water [6], which can significantly affect the glass properties such as glass transition temperature,

* Corresponding author.

E-mail address: uros.hribar@ijs.si (U. Hribar).

<https://doi.org/10.1016/j.jnoncrysol.2025.123837>

Received 19 August 2025; Received in revised form 22 October 2025; Accepted 23 October 2025

Available online 1 November 2025

0022-3093/© 2025 The Author(s). Published by Elsevier B.V. This is an open access article under the CC BY license (<http://creativecommons.org/licenses/by/4.0/>).

Table 1

Chemical composition of the used waste glasses, expressed in wt%.

	Na ₂ O	MgO	Al ₂ O ₃	SiO ₂	K ₂ O	CaO	Fe ₂ O ₃	SrO	ZrO ₂	BaO
CRT	7.7	0.3	2.4	61.0	7.1	0.8	0.2	7.8	1.5	9.7
FG	13.5	1.7	1.5	72.4	0.6	9.7	0.1	0.03	0.02	0.14
MCG	13.7	1.8	1.7	71.5	0.6	9.7	0.4	0.02	0.02	0.07

relaxation rate, and viscosity [7,8]. Water content within the glass structure can extend from a few ppb in optical fibers to several percent in natural glasses. The reaction between silicate glass and liquid water, aqueous solution, or water vapors is thus possible [9]. Water within the glass can exist in the form of OH⁻ groups and molecules, the former normally dominating at a lower and the latter at a higher total water content [10]. Use of increased pressures, i.e. autoclave reactors, can lead to incorporation of water within a glass, even at temperatures significantly below the glass transition point, where the achievable hydration quantity depends on the amount of added water, temperature, pressure, pH, and glass composition [11]. Such glass silicates are also termed hydrosilicates. It is well accepted that hydrosilicates can foam when heated, which is commonly explained as a consequence of water evaporation. Several studies have reported this phenomenon in hydrothermally treated hot-pressed glass [12–16] or hydrothermally treated glass [17]. It was recently shown that water glass can be used as a protective additive, enabling the use of carbonaceous foaming additive in the air atmosphere. Furthermore, it was also shown that newly-formed carbonate phases act as co-foaming agents, further stimulating the foaming action [18].

This investigation aims to evaluate the suitability of hydrothermally treated waste glass for the preparation of foamed glass, using a carbonaceous foaming agent, i.e. glycerol, in the air atmosphere. Use of glycerol in glass foaming requires an addition of a protective agent due to volatilization and burning of glycerol. Water glass was investigated in this regard and it was shown that initial solidification due to the addition of water glass partially prevents the volatilization of glycerol [19]. This allows for the incomplete decomposition of glycerol and formation of pyrolytic carbon which can interact with the softened glass phase at elevated temperatures to form CO and CO₂ [20]. The first part of this research focuses on foaming behavior of three types of waste glasses after being subjected to hydrothermal treatment. In the second part we focus on the ability of hydrated glass powders in enabling the effective use of glycerol as a glass foaming additive in the air atmosphere. Successful implementation of such processing route presents a potential for not only decreasing the required processing temperature but also eliminating the requirement for the addition of water glass.

2. Methodology

The chemical composition of the investigated waste cathode ray tube panels, flint and mixed color container glass (henceforth referred to as CRT, FG and MCG, respectively) is shown in Table 1. For preparing hydrous silicates, the received powders were mixed with distilled water, sealed in a pressure vessel (acid digestion vessel, with a 125 ml removable PTFE cup, Parr) and heated to 200 °C where they were kept for 12 h. Glass–water mixtures sealed in the pressure vessel contained either 10 or 30 wt% of distilled water. The hydrothermally treated glasses are further referred to as *X*_{H10} or *X*_{H30}, *X* being one of the three examined waste glass powders (CRT, FG or MCG). Note that the *X*_{H10} and *X*_{H30} labels refer to the amount of water used in sample preparation, not the actual amount incorporated into the glass structure during hydrothermal processing.

After the hydrothermal treatment, the samples became partially densified and therefore required additional processing. They were dried at 80 °C and crushed in a vibratory mill for 10 s. The milling conditions were kept constant to obtain powders with similar particle sizes as the particle size has a distinct effect on the foaming process [21]. The expansion behavior of the hydrated powders was analyzed using heating stage microscopy (HSM, EM201x, Hesse instruments). Approximately 25 mg of foaming mixture powder was manually compacted in a steel die with a diameter of 3 mm, placed onto an alumina holder, and heated to 1000 °C at 5 °C min⁻¹. The obtained images were analyzed and processed to calculate the volume of the sample via its rotational symmetry (details in Supplementary Materials). A similar amount (20–25 mg) of compressed foaming mixture was used also for thermogravimetry coupled with mass spectrometry (TG-MS, NETZCH STA 499 C/6/G Jupiterm 403 C Aeoloss QMS 403) to follow the mass changes and gas evolution during the heating. The structural changes in the samples after hydration were analyzed using X-ray diffractometry (XRD, Malvern PANalytical Empyrean diffractometer, Cu-K_α radiation source, *l* = 1.54187 Å, 45 kV and 40 mA). PDF-5 database was used to analyze the data obtained from the XRD measurements via HighScore Plus software. For the FTIR analysis in DRIFT mode (PerkinElmer Spectrum 100, 500–4000 cm⁻¹ range, spectral resolution of 4 cm⁻¹) the samples were

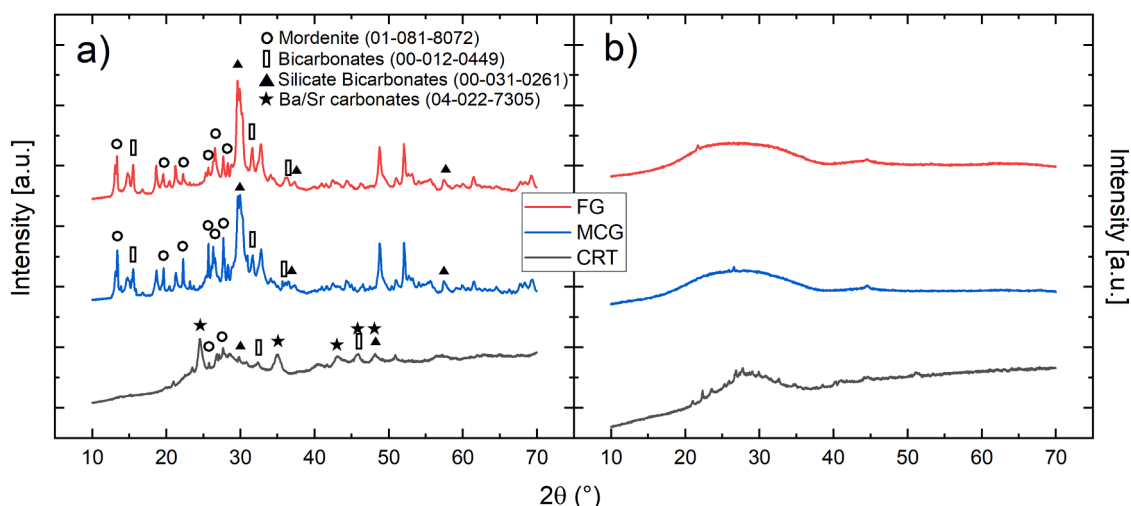


Fig. 1. X-ray diffraction data of CRT_H30, MCG_H30 and FG_H30 glass powders (a) before and (b) after the heat treatment at 800 °C.

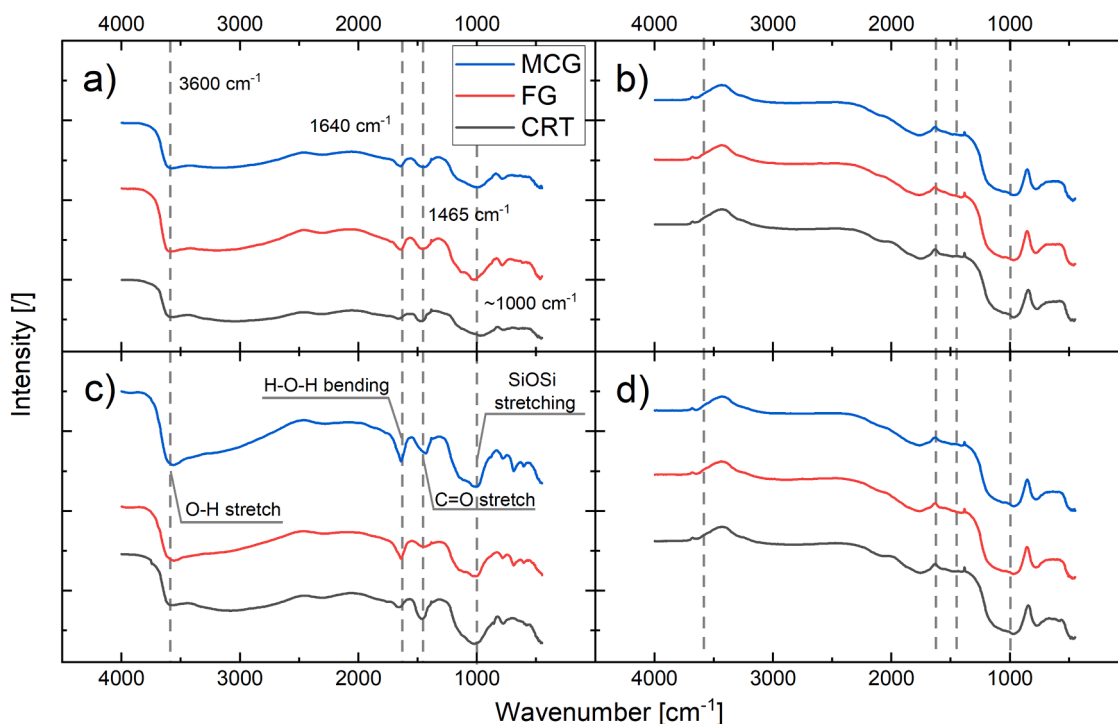


Fig. 2. FTIR of hydrothermally treated glass powders: a) 10 wt% of water, b) 10 wt% of water after treatment at 800 °C, c) 30 wt% of water, and d) 30 wt% of water after treatment at 800 °C.

mixed with potassium bromide in a 1:100 ratio (sample:KBr). XRD and FTIR analysis was implemented before and after the hydrothermal treatment to detect the structural changes in the glass powders.

Foam samples were prepared by compacting the hydrothermally treated powders (~1 g) in a stainless-steel mold ($\phi 12$) with 30 MPa and heat-treating them for 5 min in the air atmosphere. Foamed glass samples were prepared at T_{foam} where the majority of the shrinkage or expansion behavior was observed, i.e. at 600, 700, 800, and 900 °C (with 5 °C/min). After, the samples were rapidly cooled to 550 °C from where they were slowly cooled down to room temperature. The apparent density of the foamed glass samples was determined by Archimedes principle (in deionized water), and their pycnometric density was measured with a helium gas pycnometer (He, Ultracyc 5000 Foam).

In the first part of the investigation, the foaming behavior of hydrated glass powders was investigated with respect to their composition and hydration amount. In the second part, the effect of particle size was investigated by additionally milling the hydrothermally treated powders for various times (5, 20, or 60 min) in a planetary ball mill (PM 200, Retsch) and manually mixing them with glycerol (1.2 wt%). Industrial-grade glycerol with purity >99 % was used. Note, that glycerol addition was always performed after the milling.

3. Results and discussion

3.1. Characterization of hydrothermally treated CRT, MCG and FG powders

After the hydrothermal treatment, the initially amorphous glass powders became partially crystalline (Fig. 1a). Following heat treatment at 800 °C, all powders reverted to an amorphous state (Fig. 1b), indicating that the majority of the crystalline phases present in the hydrothermally treated samples are not stable at elevated temperatures. The crystalline phases identified in the case of CRT_H30 powder best coincide with diffraction data for Sr- and Ba-based (bi)carbonates. The FG_H30 and MCG_H30 signals are very similar, best matching references

for the silicate alkali carbonate hydrates, magnesium/aluminum silicate, and zeolite mordenite. However, due to the complex pattern of the multiple phases and/or low peak intensities, it is not possible to confirm the presence of all phases. Few other investigations on hydrothermal treatment of similar waste glasses do report on the formation of zeolites [17,22]. All crystalline phase signals disappear after the heating to 800 °C, which benefits foaming efficiency since crystallization usually has a negative influence on the foaming process [23].

All hydrothermally treated powders contain OH⁻ and CO₃²⁻ groups (Fig. 2a and c), which disappear after the heat treatment at 800 °C (Fig. 2b and d). The distinct peaks at ~1640 cm⁻¹ and ~1465 cm⁻¹ are related to H₂O bending [24] and CO₃²⁻ groups, respectively [25]. The powders also exhibit a strong signal at ~3600 cm⁻¹ (Fig. 2a and c) related to OH stretching of a SiOH active group [24]. This signal continues into a wide band (3500–2200 cm⁻¹), without distinct peaks, related to the OH⁻ stretching modes of H₂O active groups, indicating the presence of H₂O in various interactions with the glass network [26]. A wide signal at ~1000 cm⁻¹ and a narrower signal at ~780 cm⁻¹ are related to stretching within the glass network tetrahedra and bridge stretching between the tetrahedra, respectively [27,28]. Additionally, two less intense signals appear at ~680 and ~600 cm⁻¹ for the X_H30 glass powders (Fig. 2c). While the 780 cm⁻¹ signal is present for all the glasses, only FG_H30 and MCG_H30 exhibit more pronounced signals at 680 and 600 cm⁻¹, indicating their similarity. These two peaks could likely indicate the presence of similar crystalline phases in FG and MCG glasses after the hydrothermal treatment. After the heat treatment, the OH⁻, H₂O, and carbonate-related signals disappear, consistently with the XRD results, while the relative intensity of the signals, belonging to the glass network, increases (Fig. 2b and d).

The analysis of the structure indicates that hydrothermally treated glass powders contain carbonates, which are well-known additives in the field of glass foaming. However, in contrast to adding carbonates to the foaming mixture, when foaming with hydrous silicates the carbonates form only when the moist powder comes into contact with the air atmosphere. The degree to which the reaction between the CO₂ from the air and hydrous silicate can proceed detrimentally affects the

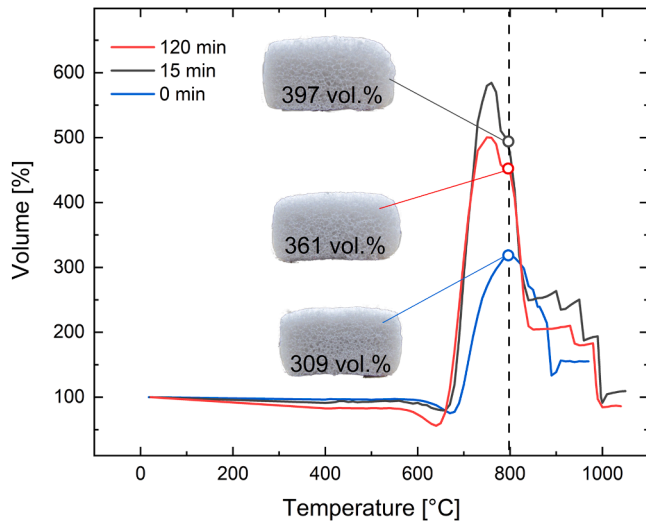


Fig. 3. Heating stage microscopy of the CRT_H10 powder samples (25 mg) milled for varying times and corresponding samples (1 g) with labelled volumetric expansion for foaming mixture treated at 800 °C.

mechanism of the foaming process as shown in the case of foaming with water glass [18]. The results above suggest that a similar foaming mechanism is in play when hydrothermally treated glass powders are implemented in glass foaming. Furthermore, according to the kinetics described in [29], the temperature of the carbonate decomposition can be modified by the milling time, consequently affecting the properties of the obtained foamed glasses. The CRT_H10 sample was thus additionally milled for 15 or 120 min at 250 rpm with the aim of achieving three significantly different particle size distributions. The dependence of the CRT_H10 on milling time is shown in Fig. 3, showing an initial increase and then a decrease in the sample volume with milling time. Samples prepared from additionally milled mixtures were foamed at 800 °C and are shown in Fig. 3. Note that some discrepancy in volume can occur between the heating stage microscopy results (25 mg samples) and foamed glass samples (1 g samples) due to the difference in sample size and contraction during the cooling of the 1 g samples. An optimum milling time thus exists and depends on the relation between the carbonate decomposition kinetics and the sintering behavior of the glass powder [29].

3.2. Expansion behavior of the hydrothermally treated CRT, MCG and FG powders

The behavior of the X_H10 and X_H30 glass powders during heating was investigated using the heating stage microscope and TG/MS. Hydrothermal treatment clearly affects heating behavior, as untreated powders (CRT, MCG, FG) show no significant expansion (Fig. 4). Among the raw glass powders, CRT glass exhibits the lowest sintering temperature (T_{sint}) which is likely the reason why also CRT_H10 and CRT_H30 exhibit lower foaming temperatures (T_{foam}) in comparison to MCG and FG glass powders. Additionally, CRT_H10 and CRT_H30 also achieve higher maximum expansion values (Fig. 4 and Table 2). The expansion stage of MCG_H10 and FG_H10 begins at a similar temperature, but FG_H10 expands less. Higher water content clearly affects the behavior of all powders during the heat treatment since the X_H30 samples, which theoretically contain 30 wt% of H₂O, exhibit smaller shrinkage and larger expansion in comparison to X_H10 samples (Fig. 4 and Table 2). However, the degree to which the hydrothermal treatment affects the behavior of glass powders during heating differs between the different powders. The increase in expansion is most pronounced for the CRT glass, while it is comparable for the MCG and FG glass powders. The decrease in characteristic temperatures with a higher water content is in accordance with the effect of structurally bound water and increased partial pressure of water on the viscosity and sintering behavior of glass powders [30,31].

For the 10 wt% hydrated samples, TG/MS shows distinct mass loss below the sintering temperature, accompanied by strong H₂O release (Fig. 5). The measured mass losses were 9.3, 7.9, and 6.6 wt% for CRT_H10, FG_H10, and MCG_H10, respectively, which are slightly lower than the theoretical 10 wt% due to partial evaporation before analysis. Water release continues up to ~600 °C, resembling behavior reported for glass-water glass mixtures [5,18]. In addition, a second signal

Table 2

Sintering temperature (T_{sint}), foaming temperature (T_{foam}), collapse temperature (T_{collapse}), and maximum volume (V_{max}) of the raw and hydrothermally treated CRT, MCG, and FG glasses.

		T_{sint} [°C]	T_{foam} [°C]	T_{collapse} [°C]	V_{max}
CRT	Raw	600	/	/	100
	H10	616	675	836	319
	H30	/	595	795	587
MCG	Raw	639	/	/	100
	H10	646	705	905	247
	H30	/	655	935	281
FG	Raw	642	/	/	100
	H10	662	725	905	160
	H30	/	660	955	215

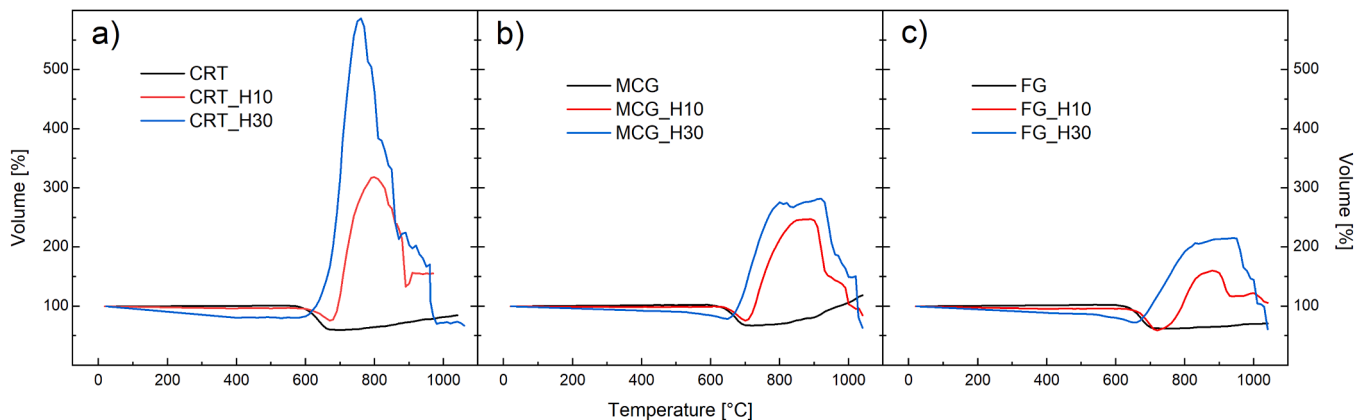


Fig. 4. Sintering and expansion behavior of raw and hydrothermally treated a) CRT, b) MCG, and c) FG powders. The suffix “_HX” denotes the theoretical wt% (X) of water within the powder.

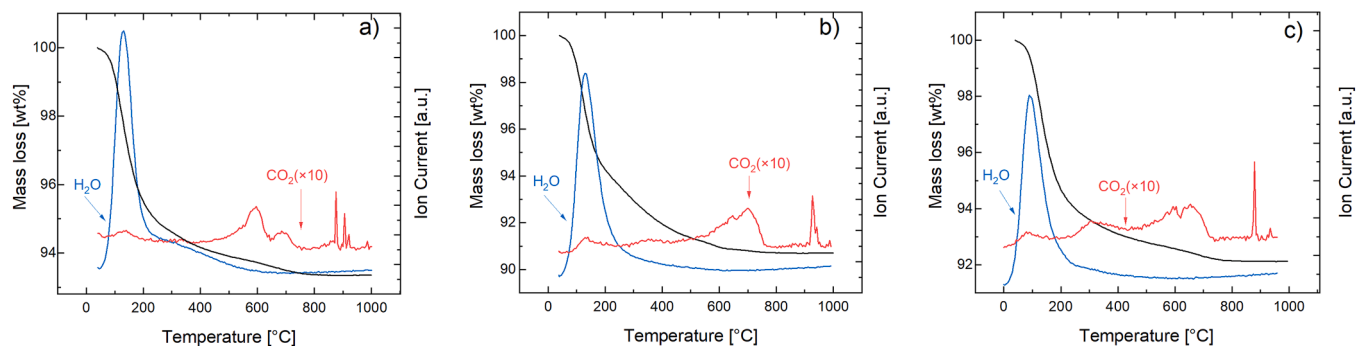


Fig. 5. Mass loss and evolved gas signals for the a) CRT_H10, b) FG_H10, and c) MCG_H10 powders during the heat treatment.

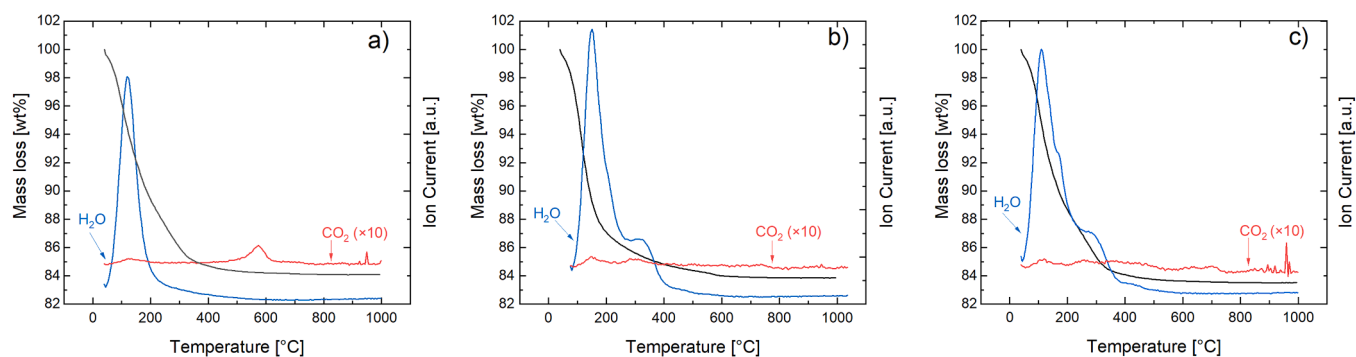


Fig. 6. Mass loss and evolved gas signals for the a) CRT_H30, b) FG_H30, and c) MCG_H30 powders during the heat treatment.

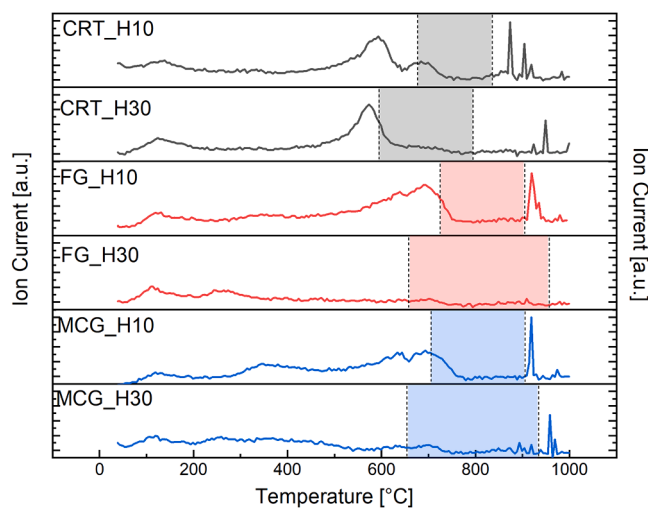


Fig. 7. Comparison of the MS data for CO₂ of all the samples (from Fig. 5 and Fig. 6) with the stable foaming range marked for each specific composition (from Fig. 4).

appears at ~ 550 – 600 °C, marking CO₂ evolution from carbonate decomposition. This indicates the presence of carbonate phases formed by the reaction between hydrated silica and atmospheric CO₂, in agreement with the XRD and FTIR results (Fig. 1 and Fig. 2). The onset of decomposition occurs at ~ 550 °C for CRT_H10 (Fig. 5a) and slightly higher (~ 600 °C) for FG_H10 and MCG_H10 (Fig. 5b and c), reflecting differences in glass composition and carbonate stability [32]. At temperatures > 800 °C, sharper and more intense CO₂ signals emerge, corresponding to the rupture of large pores and the rapid release of trapped gases.

For the samples hydrated with 30 wt% of water, mass losses of 15.9,

16.1, and 16.5 wt% were recorded (Fig. 6) for CRT_H30, FG_H30, and MCG_H30, respectively, which is significantly lower than the theoretical value of 30 wt%. This confirms that only part of the added water is structurally incorporated, while the rest condenses on the surface of the powders and easily evaporates during drying or early heating. As in the X_H10 samples, H₂O release extends up to ~ 600 °C, whereas in the case of FG_H30 and MCG_H30 the water release is less continuous, consistent with the formation of hydrated crystalline phases (Fig. 1a). CO₂ evolution occurs in the case of X_H30 samples as well, but at lower intensity than in the X_H10 series. This suggests that higher water content shifts the sintering stage to lower temperatures, enhancing the gas entrapment.

A further look into the evolution of CO₂ can clarify the expansion behavior of the hydrothermally treated glass powders. CRT_H10 exhibits two wide peaks for CO₂ gas signal in the range of 500–800 °C, while for the CRT_H30 only the lower-temperature peak can be observed (Fig. 7). This change can be attributed to the effect of a higher H₂O content on the shift of the sintering stage to lower temperatures (shaded area in Fig. 7). Consequently, due to the shift of the sintering stage to lower temperatures, more CO₂ gas, which evolves with the carbonate decomposition, can become entrapped in the material. Therefore, the second CO₂ peak, observed in the case of the CRT_H10 sample, cannot be seen in the case of the CRT_H30 composition. The shift of the sintering stage to the lower temperatures can also explain the absence of CO₂ peaks in the 500–800 °C range for the FG_H30 and MCG_H30 compositions, while the peaks are present for their counterparts with less water, i.e. FG_H10 and MCG_H10 (Fig. 7). Foam collapse is indicated by sharp CO₂ peaks, caused by the breaking of the surface pores. These peaks do not appear within the region where the sample is stable and expanding (the marked shaded area in Fig. 7). Note, that sharp CO₂ peaks do not appear for the FG_H30 sample which could be due to its good stability at high temperatures (Fig. 4), meaning that a higher temperature would be needed for the collapse of the foam and appearance of the peaks.

Hydrothermally treated waste glass powders were treated in a

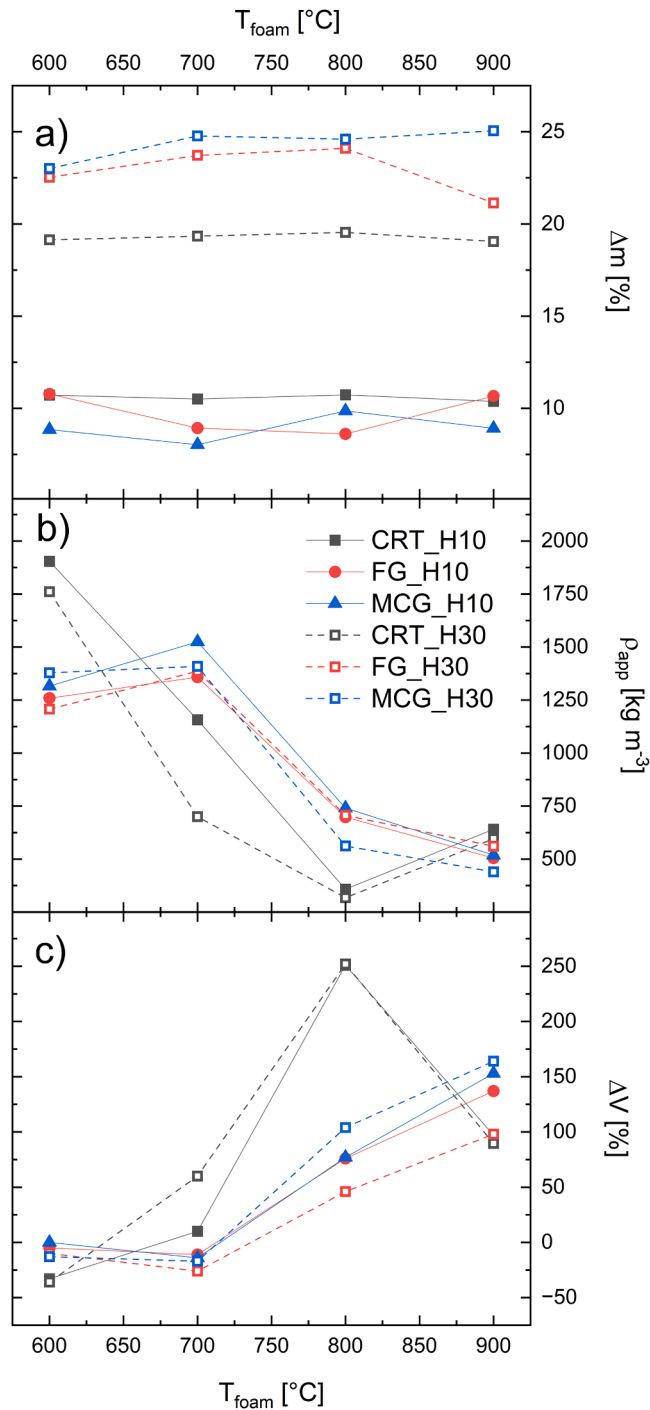


Fig. 8. a) Mass loss – Δm , b) apparent density – ρ_{app} , c) and calculated volumetric expansion – ΔV – for the foam samples prepared from hydrothermally treated glass powders after the vibration mill (10 s).

vibration mill for 10 s, shaped into 1 g pellets, and then foamed for 5 min at various foaming temperatures (Fig. 8). As shown in Fig. 8, foams prepared from the powders with a higher content of water (X_{H30}) exhibit larger difference between their mass before and after the heat treatment (mass loss, Δm) in comparison to the powders with a lower content of water (X_{H10}). The effect of the foaming temperature (T_{foam}) on the Δm is small. All the X_{H10} samples exhibit fairly similar Δm of 6–10 wt%, while the X_{H30} samples exhibit more variability (18–25 wt %) in Δm with respect to the glass type. Additionally, the Δm of the X_{H30} samples is significantly smaller than the actual amount of added

H_2O during the hydrothermal treatment of glass powders, i.e. 30 wt%. Both observations are related to the ability of a specific glass composition to form hydrosilicates. A higher content of incorporated water, whether in molecular- or SiOH -form, is expected in the case of FG and MCG glasses since water dissolution in glass increases with the content of alkalis, while alkaline earth ions inhibit the formation of hydrosilicates [9]. Note, that while CRT glass does contain hydration-promoting Na and K it also contains high content of inhibiting alkaline earths (Ba and Sr). As observed with HSM (Fig. 4), CRT-based samples start to expand at the lowest temperature and exhibit the most pronounced volume change ($\Delta V = 1 - V_{\text{after}}/V_{\text{before}}$ in Fig. 8). FG-based samples on the other hand exhibit the lowest ΔV . Both, CRT_H10 and CRT_H30 reach a similar maximum ΔV in Fig. 8, in contrast to observations with HSM (Fig. 4).

All of the hydrothermally treated glass powders form a porous structure when heat-treated. Foaming of hydrothermally treated glass powders begins below 750 $^{\circ}\text{C}$, and shifts to even lower temperatures with increasing water content. In all glass powders, water release is observed upon heating, while at higher temperature CO_2 evolution is also detected. The sharp CO_2 signals at elevated temperatures indicate its role in the foaming process. Based on these results, we propose that the main foaming mechanism is related to the formation of carbonates on the surface of hydrated particles. Furthermore, incorporation of water into the glass structure affects its thermomechanical properties by lowering both viscosity and characteristic transition temperatures. The combination of both effects causes part of the carbonate decomposition to occur only after the material structure has already closed. The decomposition products (CO_2) are then trapped within the sintered matrix and subsequently act as the driving force for foaming. The foaming mechanism of hydrothermally treated glass is therefore very similar to that of a mixture of glass and water glass [18]. 800 $^{\circ}\text{C}$ appears to be in the vicinity of the optimal T_{foam} for the FG_HX and MCG_HX powders, where the samples expand the most. For the CRT_HX powders, 800 $^{\circ}\text{C}$ already appears to be slightly above their optimal T_{foam} . All further experiments, testing the applicability of hydrothermally treated glass powders for foaming with glycerol in the air atmosphere, were implemented at 800 $^{\circ}\text{C}$ for better comparability between the compositions.

3.3. Effect of additives on foaming with hydrothermally treated glass powders

Glass foaming with carbonaceous foaming additives can be achieved in air if the carbon is protected from premature burning, e.g. with water glass [5]. Here we investigated whether a similar outcome can be achieved with the use of hydrothermally treated glass powder in combination with glycerol. For this purpose, we added 1.2 wt% of glycerol to the hydrated glass. Additionally, we inspected the influence of the particle size on the process dynamics and maximum achieved expansion (Fig. 9).

Additional milling of hydrothermally treated FG and MCG glasses significantly improves their expansion during heating (Fig. 10). Reducing the mean particle size decreased the apparent density from $> 600 \text{ kg m}^{-3}$ for MCG and FG, to $< 200 \text{ kg m}^{-3}$. The density of CRT_H30 shows little dependence on particle, likely because 800 $^{\circ}\text{C}$ is above its optimal T_{foam} (Table 2), and further milling might shift the expansion and collapse stages to even lower temperatures. A decrease of the particle size thus not only result in a downward shift of the T_{sint} and T_{foam} , but also in a downward shift of T_{collapse} for the CRT_H30 sample.

The structure analysis indicates that hydrothermally treated glass powders contain carbonates (Fig. 1 and Fig. 2). According to the carbonate decomposition kinetics and their effect on glass foaming [29], the temperature of the decomposition can be modified by the milling time, consequently affecting the properties of the obtained foamed glasses. It was shown that an optimum milling time, which results in maximum possible expansion, exists.

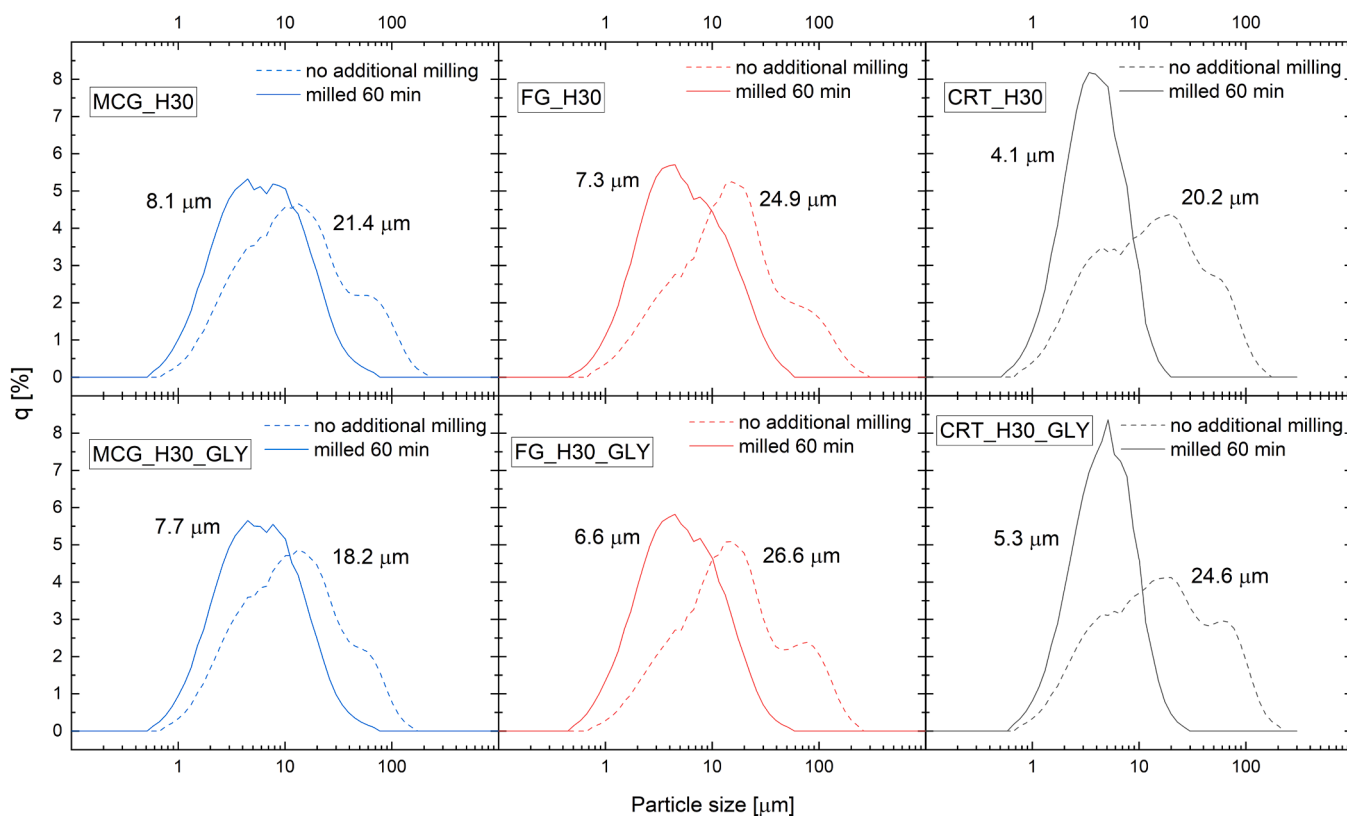


Fig. 9. Particle size distribution of the investigated glass types for no additional milling and after additional milling for 60 min in a planetary ball mill. The mean particle size is labelled next to each distribution curve.

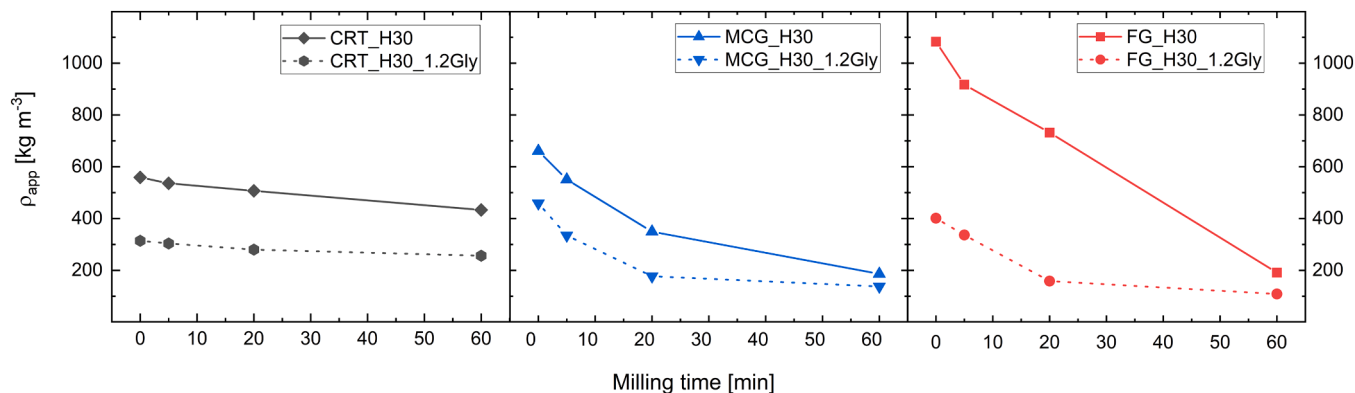


Fig. 10. Apparent density of the foamed glass samples obtained from hydrothermally treated CRT, MCG, and FG glass powders, foamed at 800 °C.

The effect of improved expansion as a consequence of additional milling is also observed if foaming mixtures contain glycerol (Fig. 11). Furthermore, addition of glycerol to hydrosilicates results in foams with significantly lower density. Interestingly, the color of the glycerol-containing samples changes with milling time, i.e. with decreasing particle size. The change in the sample color with increasing milling time thus suggests that a higher content of carbon becomes trapped within the material which could be a consequence of decreasing $T_{\text{ sint}}$. Darkening of the sample color was already observed in the research of glass foaming [19,33] and was attributed to higher content of unburned carbon from the glycerol. Addition of glycerol and adjustment of particle size distribution results in highly porous samples, most noticeable for *FG_H30* and *MCG_H30* powders, which is a desired feature in thermal insulation materials.

To further evaluate the compositions that have demonstrated

promising properties, we prepared larger samples which will serve as an initial assessment of the materials' practical applicability as a thermal insulation material and the rationale for pursuing further investigations. Glycerol-containing mixtures of *MCG_H30* and *FG_H30*, milled for 60 min, were chosen for this purpose. The powder processing and thermal treatment (800 °C) were kept identical with the exception of the holding time, which was prolonged to 20 min. The appearance of the larger samples, their crystallinity, and pore size distribution are shown in Fig. 12. An apparent density (ρ_{app}) of 190 and 175 kg m⁻³ was achieved for *MCG_H30* and *FG_H30* samples, respectively. Such ρ_{app} of large samples is higher than the ρ_{app} of the corresponding smaller samples (Fig. 10) which can be attributed to the higher content of crystalline phases (Fig. 12b). Both samples are more crystalline than corresponding hydrosilicates after the heat treatment, with quartz, cristobalite and sodium/calcium silicate as the main phases (PDF codes 01-083-0539,

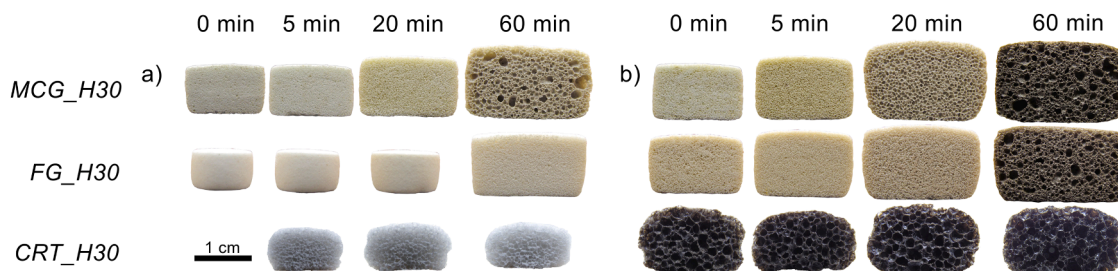


Fig. 11. Images of the foamed glass samples prepared at 800 °C ($t_{\text{foam}} = 5$ min) from hydrothermally treated glass powders a) without and b) with the addition of glycerol (1.2 wt%), milled in a ball mill for a labelled amount of time.

01-089-3607 and 00-023-0671 respectively). Crystallization of the samples in Fig. 12 is very likely related to additional milling and prolonged foaming time, since hydrothermally treated FG and MCG powders from do Fig. 1b not exhibit significant crystallization peaks. The *FG_H30* sample exhibits larger pores (Fig. 12c) in comparison to the *MCG_H30* sample (median ferret diameter of 1.57 and 0.82 mm, respectively), which is a common trend when decreasing ρ_{app} of the latter sample.

The samples were shaped into 10 cm × 10 cm × 2 cm blocks and tested for thermal conductivity and open porosity. Open porosity of 45 and 9 % and thermal conductivity of 65 and 66 mW (m K)⁻¹ were achieved for the *MCG_H30* and *FG_H30* compositions, respectively. The measured thermal conductivity values are higher than those of commercially available foamed glass boards ([3,34]) which is most likely related to the observed crystalline structure. *FG_H30* sample exhibits a significantly lower content of open pores in comparison to the *MCG_H30* while their density and thermal conductivity are fairly similar. This suggests that the thermal conductivity of the trapped gaseous phase is not significantly different from the thermal conductivity of air. The balance between CO and CO₂ as well as the formation of H₂ can significantly affect the conductivity of the gaseous phase.

Although the thermal conductivity of the obtained samples is higher than desired (conventional thermal insulation materials have values below 50 mW (m K)⁻¹), the low open porosity observed in the *FG_H30* composition (below 10 vol %) is a promising attribute. This indicates the potential for further exploration of the material's peculiarities with respect to its thermal conductivity and the need for process modifications to improve its insulation performance.

4. Conclusions

This study demonstrates that hydrothermally treated waste glass can be used for synthesis of foamed glass. A higher degree of hydration decreases the powder's onset foaming temperature and promotes greater expansion. This effect is most pronounced in cathode ray tube waste glass compared to flint and mixed-color container glass, which are more susceptible to crystallization, thereby limiting their expansion.

The presence of carbonates, together with the shape of the expansion and gas-evolution curves, indicates that the foaming mechanism is similar to that observed in glass-water glass mixtures, suggesting that carbonate decomposition is the main driving force for the expansion. Extended milling of hydrothermally treated powders enhances the

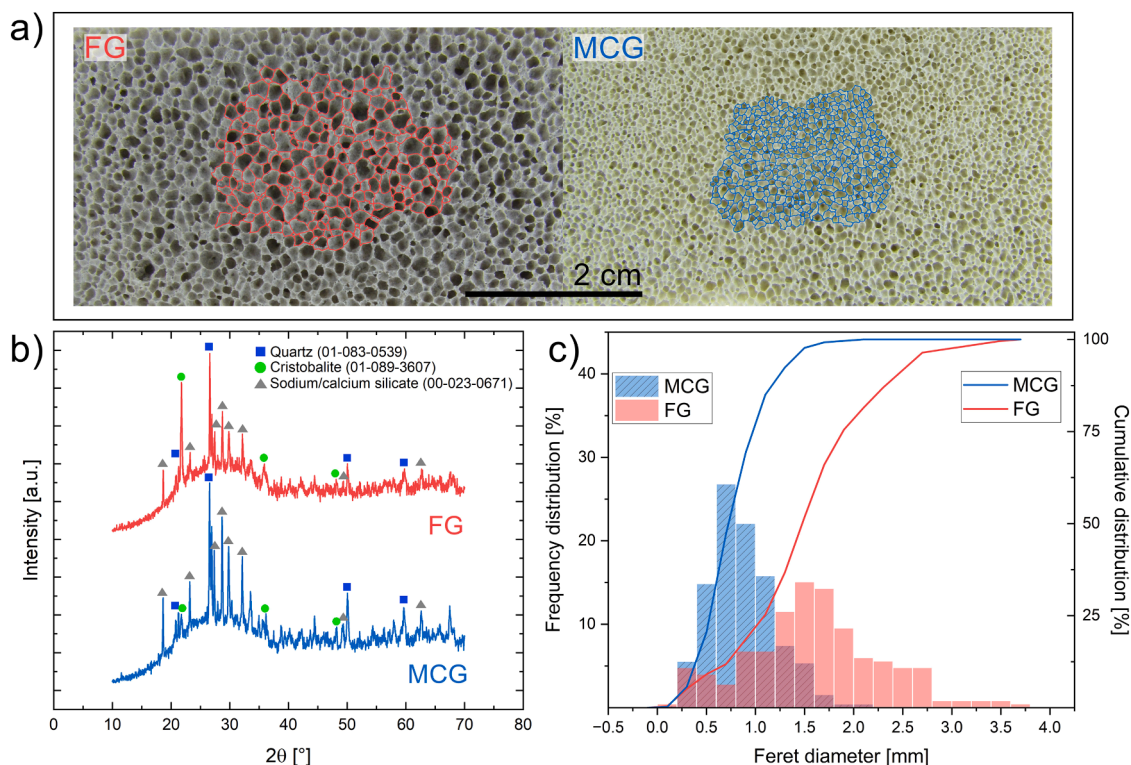


Fig. 12. a) surface appearance with an overlay of pore outlines for *FG_H30* and *MCG_H30* (with 1.2 wt% glycerol) samples foamed at 800 °C ($t_{\text{foam}} = 20$ min), b) XRD patterns, and c) pore size distribution.

expansion, yielding minimum densities of 433, 186, and 191 kg m⁻³ for CRT_H30, MCG_H30, and FG_H30, respectively. When combined with glycerol, even lower densities were achieved—256, 137, and 108 kg m⁻³ for the same glass types. Importantly, this process can be performed in air, highlighting hydrothermal treatment of waste glass as a promising alternative processing route.

Larger foams prepared from MCG_H30 and FG_H30 with glycerol showed significant differences from their smaller counterparts, most notably increased crystallinity, higher apparent densities (>175 kg m⁻³), and relatively high thermal conductivity (>65 mW m⁻¹K⁻¹). Future work should focus on understanding and mitigating crystallization during scale-up. Controlling this factor could lower density, improve thermal insulation, and expand the potential applicability of foamed glass from hydrothermally treated waste.

Data availability

Dataset from this study is available under <https://doi.org/10.5281/zenodo.14643456>.

CRediT authorship contribution statement

Uroš Hribar: Writing – original draft, Visualization, Methodology, Investigation, Formal analysis, Data curation, Conceptualization. **Matjaž Spreitzer:** Supervision, Funding acquisition. **Jakob König:** Writing – review & editing, Supervision, Resources, Conceptualization.

Declaration of competing interest

The authors declare that they have no known competing financial interests or personal relationships that could have appeared to influence the work reported in this paper.

Acknowledgements

Authors would like to thank D. Fabijan for performing the measurements with a heat flow meter and S. Zupančič for performing the measurements with a heating stage microscope. This work was supported by the Slovenian Research and Innovation Agency (Grant number P2-0091).

Supplementary material

Supplementary material associated with this article can be found, in the online version, at doi [10.1016/j.jnoncrsol.2025.123837](https://doi.org/10.1016/j.jnoncrsol.2025.123837).

References

- [1] J.H. Butler, P.D. Hooper, *Glass Waste*, 2nd ed., Elsevier Inc., 2019.
- [2] M. Scheffler, P. Colombo, *Glass Foams*, in: M. Scheffler, P. Colombo (Eds.), *Cellular Ceramics*, Wiley - VCH Verlag GmbH & Co. KGaA, Weinheim, 2005, pp. 158–176. Eds.
- [3] 'Environmental Product Declaration Foamglas W+F and T3+'.
[4] J. König, A. Lopez-Gil, P. Cimavilla-Roman, M.A. Rodriguez-Perez, R.R. Petersen, M.B. Østergaard, N. Iversen, Y. Yue, M. Spreitzer, Synthesis and properties of open- and closed-porous foamed glass with a low density, *Constr. Build. Mater.* 247 (2020) 118574. Jun.
- [5] U. Hribar, M. Spreitzer, J. König, Applicability of water glass for the transfer of the glass-foaming process from controlled to air atmosphere, *J. Clean. Prod.* 282 (2021).
- [6] R.K. Iler, *The Chemistry of Silica*, John Wiley & Sons, 1979.
- [7] S. Zietka, J. Deubener, H. Behrens, R. Müller, Glass transition and viscosity of hydrated silica glasses, *Phys. Chem. Glas. Eur. J. Glas. Sci. Technol. Part B* 48 (6) (2007) 380–387.
- [8] M. Tomozawa, Water in glass, *J. Non. Cryst. Solids* 73 (1–3) (1985) 197–204.
- [9] R.H. Doremus, *Glass Science*, 2nd ed., John Wiley & Sons, New York, 1994.
- [10] J. Acocella, M. Tomozawa, E.B. Watson, The nature of dissolved water in sodium silicate glasses and its effect on various properties, *J. Non. Cryst. Solids* 65 (2–3) (1984) 355–372.
- [11] R.F. Bartholomew, P.A. Tick, S.D. Stookey, Water/glass reactions at elevated temperatures and pressures, *J. Non. Cryst. Solids* 38–39 (Part 2) (1980) 637–642.
- [12] M. Suzuki, T. Tanaka, N. Yamasaki, Use of hydrothermal reactions for slag/glass recycling to fabricate porous materials, *Curr. Opin. Chem. Eng.* 3 (2014) 7–12.
- [13] M. Suzuki, T. Tanaka, Hydrothermal slag /glass chemistry for porous materials production, *Key Eng. Mater.* 521 (2012) 35–45.
- [14] Z. Matamoros-Veloza, J.C. Rendón-Angeles, K. Yanagisawa, M.A. Cisneros-Guerrero, M.M. Cisneros-Guerrero, L. Aguirre, Preparation of foamed glasses from CRT TV glass by means of hydrothermal hot-pressing technique, *J. Eur. Ceram. Soc.* 28 (4) (2008) 739–745.
- [15] Z. Matamoros-Veloza, J.C. Rendón-Angeles, K. Yanagisawa, E.E. Mejia-Martínez, J. R. Parga, Low temperature preparation of porous materials from TV panel glass compacted via hydrothermal hot pressing, *Ceram. Int.* 41 (10) (2015) 12700–12709.
- [16] T. Yoshikawa, S. Sato, T. Tanaka, Fabrication of low temperature foaming glass materials using hydrothermal treatment, *ISIJ Int* 48 (2) (2008) 130–133.
- [17] T. Takei, H. Ota, Q. Dong, A. Miura, Y. Yonesaki, N. Kumada, H. Takahashi, Preparation of porous material from waste bottle glass by hydrothermal treatment, *Ceram. Int.* 38 (3) (2012) 2153–2157.
- [18] U. Hribar, M.B. Østergaard, N. Iversen, M. Spreitzer, J. König, The mechanism of glass foaming with water glass, *J. Non. Cryst. Solids* 600 (November 2022) (2023) 0–7.
- [19] B.M. Goltsman, E.A. Yatsenko, Dynamics of foam glass structure formation using glass waste and liquid foaming mixture, *J. Clean. Prod.* 426 (September) (2023) 138994.
- [20] B.M. Goltsman, E.A. Yatsenko, Role of Carbon Phase in the Formation of Foam Glass Porous Structure, *Materials (Basel)* 15 (22) (2022).
- [21] J. König, R.R. Petersen, Y. Yue, Influence of the glass particle size on the foaming process and physical characteristics of foam glasses, *J. Non. Cryst. Solids* 447 (2016) 190–197.
- [22] Z. Yao, D. Wu, J. Liu, W. Wu, H. Zhao, J. Tang, Recycling of typical difficult-to-treat e-waste: synthesize zeolites from waste cathode-ray-tube funnel glass, *J. Hazard. Mater.* 324 (2017) 673–680.
- [23] S. Smiljanić, U. Hribar, M. Spreitzer, J. König, Influence of additives on the crystallization and thermal conductivity of container glass cullet for foamed glass preparation, *Ceram. Int.* 47 (23) (2021) 32867–32873.
- [24] R.F. Bartholomew, B.L. Butler, H.L. Hoover, C.K. Wu, Infrared Spectra of a Water-Containing Glass, *J. Am. Ceram. Soc.* 63 (9–10) (1980) 481–485.
- [25] R.A. Brooker, S.C. Kohn, J.R. Holloway, P.F. McMillan, Structural controls on the solubility of CO₂ in silicate melts Part II: IR characteristic of carbonate groups in silicate glasses, *Chem. Geol.* 174 (1–3) (2001) 241–254.
- [26] T. Uchino, T. Sakka, M. Iwasaki, Interpretation of Hydrated States of Sodium Silicate Glasses by Infrared and Raman Analysis, *J. Am. Ceram. Soc.* 74 (2) (1991) 306–313.
- [27] R. Hanna, Infrared Absorption Spectrum of Silicon Dioxide, *J. Am. Ceram. Soc.* 48 (11) (1965) 595–599.
- [28] J.R. Ferraro, M.H. Manghnani, Infrared absorption spectra of sodium silicate glasses at high pressures, *J. Appl. Phys.* 43 (11) (1972) 4595–4599.
- [29] J. König, R.R. Petersen, Y. Yue, Influence of the glass-calcium carbonate mixture's characteristics on the foaming process and the properties of the foam glass, *J. Eur. Ceram. Soc.* 34 (6) (2014) 1591–1598.
- [30] I. Cutler, Effect of Water Vapor on the Sintering of Glass Powder Compacts, *J. Am. Ceram. Soc.* 52 (1) (1969) 11–13.
- [31] R.F. Bartholomew, *Water in Glass*, 22, Academic Press, INC, 1982.
- [32] R.V. Siriwardane, J.A. Poston, C. Robinson, T. Simonyi, Effect of additives on decomposition of sodium carbonate: precombustion CO₂ capture sorbent regeneration, *Energy and Fuels* 25 (3) (2011) 1284–1293.
- [33] P. Sooksaen, P. Thongyong, Physical and Thermal Characteristics of Expanded Foam Glasses Using Crude Glycerol As a Foaming Agent, *Suranaree J. Sci. Technol.* 30 (3) (2023) 1–9.
- [34] 'Environmental Product Declaration Glapor'.